



LUND
UNIVERSITY

SMHI

Kinetic Energy of Storms in Different Reanalysis Data Sets and Observations

Erik Höjgård-Olsen

Department of Physics at Lund University

and

SMHI

Supervisor: Heiner Körnich, SMHI

2nd supervisor: Elna Heimdal Nilsson, Lund University

Report handed in the 20th May 2014

Abstract

Storms cause severe damages and cost lives. In order to assess the severity of storms, historical data sets such as reanalysis data can be employed. This kind of data is based on numerical weather prediction models. The realism of model data is limited by the spatial resolution of the model. A numerical weather prediction model is only as precise as its grid distance, meaning that a model cannot detect phenomena occurring on scales smaller than the grid distance of the model. In this study it was investigated whether a data set using a tighter grid distance detects more weather information than one with a wider grid distance. The investigation focused on wind speeds. In order to see how well data sets using different grid distances performed for near surface wind speed, data was extracted from a few days before to a few days after three Swedish storms. The storms were Gudrun (January 2005), Per (January 2007) and Carola (December 1999). The data sets compared were ERA-Interim (80 km grid distance) and the two data sets of the EURO4M project; HIRLAM (22 km grid) and DYNAD (5 km grid). The results showed that the theoretical assumption – that the data set using the tightest grid distance detects the largest values for wind speed – only holds for events of particularly strong winds. During events of lower wind speeds the wind- and kinetic energy representations of the data sets are not ordered as expected according to the theoretical assumption. Observations from one station (Falsterbo) were compared with the kinetic energy representations of the data sets. The results showed that the data sets often overestimated the kinetic energies with respect to the observations. The station chosen was Falsterbo and it turned out to be a poor selection because the models parameterise Falsterbo to be located in the ocean when in fact it lies on a slim peninsula. Lastly, a significance test showed that, with a 95 % confidence level, the average difference in mean kinetic energy between two data sets is not zero, meaning that there is a difference between the data sets. In conclusion, it might still be that the hypothesis is correct, but then it could not be proven with this study.

Table of Content

1. Introduction
 - 1.1 Model Descriptions
 - 1.2 Aim
2. Theory
 - 2.1 The Kinetic Energy Spectrum of the Atmosphere
 - 2.2 Theory Behind the Hypothesis
 - 2.3 Data Analysis
 - 2.4 The Storms Gudrun, Per and Carola
3. Method
4. Results
 - 4.1 Development of the 2005 Storm Gudrun
 - 4.2 Kinetic Energy Representations
 - 4.3 Observation Comparisons
 - 4.4 Mean Kinetic Energy- and Theoretical Calculations
 - 4.5 Kinetic Energy
 - 4.6 Significance Test

- 5 Discussion
 - 5.1 Figures Describing Kinetic Energy Representations
 - 5.2 Observation Comparisons
 - 5.3 Mean Kinetic Energy, Variance and Significance Test
 - 5.4 Criticism of References Used
- 6 Conclusion
- 7 References

1. Introduction

The processes that maintain the atmospheric kinetic energy spectrum are not as well known today as many would like to believe. However, since Nastrom et al.'s (1984) publication, the actual spectrum is rather robustly known. It is difficult to determine all the properties of the atmosphere and the reason is that the atmosphere is a non-linear dynamic system in chaos. Thus, many approximations and parameterisations must be made to fill in the blanks in the models.

Storms cause severe damages and cost lives. In order to assess the severity of storms, historical data sets such as reanalysis data can be employed. This kind of data is based on numerical weather prediction (NWP) models. In this study it was investigated whether a reanalysis data set using a tighter grid distance detects more weather information than one using a wider grid distance. A reanalysis is a combination of a model, observations and data assimilations over a long time. It is thus not a freely running model, but a statistically derived best estimate of the atmosphere. The data sets used to execute the study are ERA-Interim (80 km grid distance), HIRLAM (22 km grid distance) and DYNAD (5 km grid distance).

The models contained within the data sets used in this study assume an atmosphere in hydrostatic balance. The assumption of hydrostatic balance means that all convective phenomena must be parameterised. The realism of model data is limited by the spatial resolution of the model. A NWP-model is only as precise as its grid distance. That is to say that the accuracy of a model is highly dependent on its grid distance. The grid distance is the distance between two grid cells. A model can only catch phenomena on scales larger than its own grid distance. In fact, a model needs several grid cells in order to describe phenomena. Thus, a tighter grid distance enables a model to catch meteorological phenomena occurring on smaller scales. The kinetic energy spectrum of the atmosphere is rather well known and could be applied to reanalysis data at different resolutions.

Next follows the general descriptions of the data sets used in this study. Then, in the second section, the Theory section, the theory behind the atmospheric kinetic energy spectrum will be described. After the Theory section comes the Method section where the study is described and next after that follows the Result section where it is deemed whether the study gave the expected results or not. After the results have been presented they are discussed in the Discussion section together with the general validity of the study. Finally, conclusions are drawn from the study and examples on future studies are suggested in the Conclusion section. Lastly, the references are listed in alphabetical order in the Reference section.

1.1 Model descriptions

In this study the regional HIRLAM and DYNAD data sets of the EURO4M project were used in comparison to the global ERA-Interim data set.

1.1.1 ERA-Interim

Over the years the European Centre of Medium-Range Weather Forecasts (ECMWF) has produced three different reanalysis models. The first two are the ones called ERA-15 and ERA-40. ERA-40 was a global model describing the state of the atmosphere and the ocean- and land conditions. It contained data from 1957 to 2002. Whilst waiting for a new and more accurate model another one was needed in the meantime. That data set is the ERA-Interim reanalysis. It is a global data set with a grid spacing of 80 km in the horizontal direction and 60 vertical levels. It contains data from 1979 to the present time (<http://www.ecmwf.int/research/era/do/get/era-interim>, 2014-04-14).

1.1.2 EURO4M

EURO4M is an EU funded project put together to provide a historical weather data set with better and more accurate state and evolution of the European climate than previous data sets. In EURO4M, several models were used, e.g. SMHI contributed with a set-up of the HIRLAM model. In this study the regional HIRLAM data set (with a 22 km grid distance) and the DYNAD data set (5 km grid) were compared with ERA-Interim. HIRLAM and DYNAD spans horizontally over Europe, the North western parts of the Atlantic Ocean, Greenland and the most northern parts of Africa, as can be seen in Figure 1 (below). In the EURO4M project the data is gathered from satellite observations and ground based stations in order to create a regional reanalysis (<http://www.euro4m.eu/>, 2014-04-03).

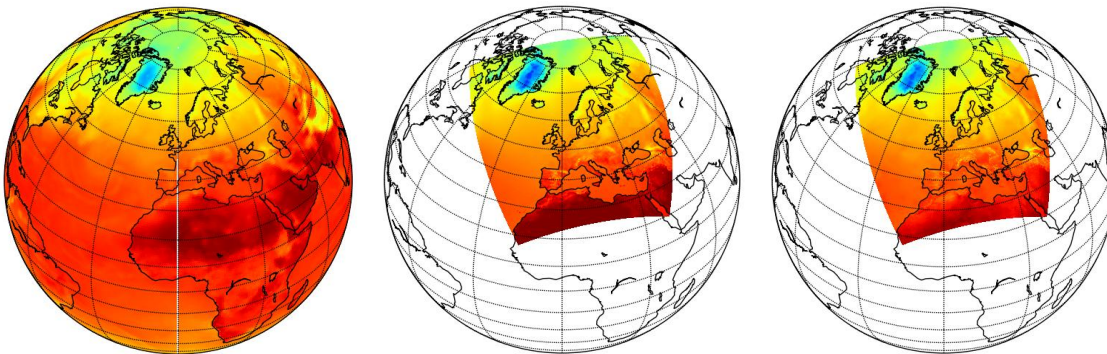


Figure 1: The figure displays the horizontal domains of ERA-Interim, HIRLAM and DYNAD from left to right.

HIRLAM in EURO4M

The HIRLAM model is a regional NWP-model. As part of the EURO4M project it has 326 grid points in the west-to-east direction and 341 grid points in the north-to-south direction. Its horizontal region is displayed in Figure 1. It both uses ERA-Interim as boundary conditions and assimilates it in its central part (Dahlgren et al., 2014).

1.1.3 DYNAD in EURO4M

DYNAD stands for DYNamic ADaptation and is a dynamical downscaling model based on HIRLAM for the 10 meter winds. To construct DYNAD, HIRLAM is downscaled and

dynamically adapted to the orography on the 5 km grid. In Figure 1 (above) the domain of DYNAD is displayed (Dahlgren et al., 2014).

1.2 Aim

The three datasets DYNAD, HIRLAM and ERA-Interim, with their respective grid distances of 5, 22 and 80 kilometres, are not expected to give the exact same output. It is reasonable to assume that the tighter the grid distance the more atmospheric information would be detected by the model. Thus, the hypothesis of this study has been formed around the relation of equation E1 below:

$$E_{kin_{ERA-Interim}} < E_{kin_{HIRLAM}} < E_{kin_{DYNAD}} \quad (E1)$$

The equation is a very simple relation stating that ERA-Interim (80 km grid) is expected to detect less kinetic energy of the atmospheric energy spectrum than HIRLAM (22 km grid), which in turn is expected to detect less kinetic energy than DYNAD (5 km grid).

In this study it was to be examined whether the relation assumed in equation E1 above was correct or not. Of course the general aim that followed from that hypothesis was also to evaluate how well the different data sets capture the storms in terms of kinetic energy. That was made by comparisons between the data sets and observations.

The events used to execute the study were the winds of the storms Gudrun, Per and Carola that hit Sweden in January 2005, January 2007 and December 1999 respectively. They were reanalysed with the datasets ERA-Interim, HIRLAM and DYNAD and compared with observations made during the storm at the station Falsterbo.

2. Theory

2.1 The kinetic energy spectrum of the atmosphere

Over the fifties and sixties, Kraichnan (1967) developed a theory describing two-dimensional turbulence. In this theory he states that eddies in a steady flow dissipate their energy into smaller eddies, which in turn dissipate their energy into even smaller ones. This dissipation of energy from large into small scale eddies continues until eddies are so small that viscosity becomes important. Then the energy of the smallest eddies dissipate into heat (Kraichnan, 1967).

When constructing his theory, Kraichnan (1967) imagined a Fourier space. In the Fourier space, turbulence was created by a random force around large wavenumbers (i.e. small wavelengths), whereas the resolution of the physical system determined the smallest wavenumbers. In Kraichnan's (1967) image, the force provides the system with both energy and enstrophy (two quantities that must both be conserved). Enstrophy is defined as half the surface integral over the vorticity, η , squared in a velocity field u .

$$\varepsilon(u) = \frac{1}{2} \int \eta^2 dS \quad (E2)$$

Kraichnan (1967) demonstrated that enstrophy and energy propagates in opposite directions to each other, meaning that as energy is propagating from large to small scales the enstrophy propagates from small to large scales. For large Reynolds numbers, inertial forces dominate over viscosity. In the region of 10^1 to 10^2 km wavelength the flow of the energy spectrum is only determined by one variable, namely the rate Π_u . Π_u is the rate at which the energy propagates through the spectrum (Lindborg, 1998).

$$E(k) = C_0 |\Pi_u|^{2/3} k^{-5/3} \quad (\text{E3})$$

In equation E3, C_0 is a dimensionless constant. The absolute value of Π_u is taken since a negative sign would indicate a flux towards small wavenumbers. The Reynolds number is defined in equation E4 (below). The Reynolds number is abbreviated “Re” and it is the ratio between inertia and viscosity. Inertia tends to maintain the motion of a fluid whilst viscosity works in a decelerating manner. At high Reynolds numbers ($\text{Re} \gg 1$) the advective acceleration is much greater than the viscous term, thus inertia dominates over viscosity. Analogously, for low Reynolds numbers ($\text{Re} \ll 1$) viscosity dominates over inertia (Lautrup, 2011).

$$\text{Re} \approx \frac{|(\mathbf{v} \cdot \nabla)\mathbf{v}|}{|\nu \nabla^2 \mathbf{v}|} \quad (\text{E4})$$

In equation E4, $\nu = \eta/\rho_0$, is the constant kinematic viscosity (ρ_0 is the density of the fluid). In the range of 10^2 to 10^3 km wavelength, the properties of the energy flow are exclusively determined by the rate Π_ω at which energy propagates through the spectrum.

$$E(k) = K \Pi_\omega^{2/3} k^{-3} \quad (\text{E5})$$

In equation E5, K is, like C_0 of equation E3, a dimensionless constant (Lindborg, 1998). The ranges $10^1 - 10^2$ and $10^2 - 10^3$ km wavelength are vague to say the least. So far, no precise threshold has been found where the $10^1 - 10^2$ km-range ends and the $10^2 - 10^3$ km starts. Nevertheless, a common approximated boundary in figures and simplifications is 500 km.

Between the years 1975-1979 commercial airlines collected meteorological data during their flights in what was called the Global Atmospheric Sampling Programme (GASP). Five years later Nastrom et al. (1984) were able to construct a determination of the kinetic energy spectrum of the atmosphere from these airline data. They found different power law dependence at different scales. For the ranges 2.6 – 300 km and 1000 – 3000 km the atmospheric kinetic energy spectrum obeyed power laws of $-5/3$ and -3 respectively. Nastrom et al. (1984) believed that at the mesoscale range (2.6 – 300 km) the $-5/3$ power law describes a reversed energy cascade that goes from high to low wavenumbers in quasi-two-dimensional turbulence. Figure 2 below illustrates at which scales the different power laws are valid. Notice that these power laws are exactly the same as those calculated by Kraichnan in the mid sixties (equations E3 and E5). On the larger synoptic scale (1000 - 3000 km), the -3 power law dependence most likely describes an enstrophy cascade from low to high wavenumbers, the process of which Nastrom et al. (1984) described as geostrophic turbulence.

Smith and Yakhot (1994) suggested that, since the k^{-3} -range is quite narrow (Figure 2), it is in fact not an enstrophy inertial range, but rather an effect of the accumulation of energy that is caused by the finite size of the Earth. In Kraichnan's image only one force term was allowed to act on the small scales. In his definition the energy inertial range must appear for smaller wavenumbers than the enstrophy inertial range. However, it is actually more reasonable to imagine one small-scale force and one large-scale force. Lilly (1989) suggested that this image is the case for the atmosphere. In the intermediate region between a small-scale force, from convective and shearing instabilities at small wavelengths, and a large-scale force, originating from baroclinic instability at wavelengths of several thousands of kilometres, it is possible that a combined energy and enstrophy inertial range exists. With Lilly's (1989) theory the $k^{-5/3}$ - and k^{-3} -ranges can still be interpreted in the two-dimensional turbulence theory (Lindborg, 1998).

2.2 Theory behind the hypothesis

Theoretically, it would be reasonable to assume equation E1 to be correct. The theory is quite simple: the tighter the grid distance, the more energy would be detected. Figure 2 (below) is an approximate drawing made to illustrate the theory that lies behind equation E1.

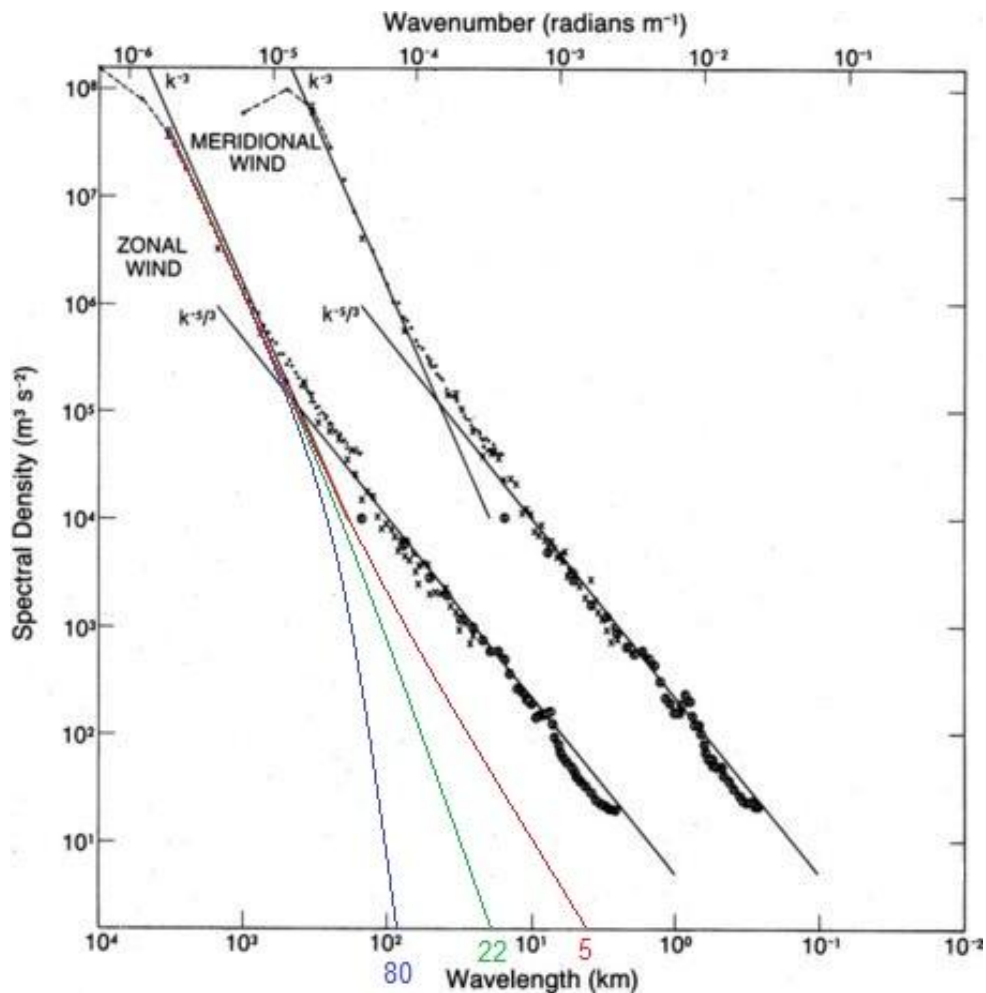


Figure 2: The black curves in the figure display the kinetic energy spectrum of the atmosphere, as found by Nastrom et al. (1984), near the tropopause with GASP aircraft data. The spectrum of the meridional wind is shifted one decade to the right (Figure reproduced from Nastrom et. al, Journal of Atmospheric Sciences, 1985, © AMS). The coloured curves are an illustration of the relations of equation E1. They are schematic interpretations of how it should look. The coloured lines go down to their respective grid distances. The ERA-Interim model (80 km grid) is represented by the blue line, the HIRLAM model in EURO4M (22 km grid) is represented by the green line and finally

The first thing that should be commented in Figure 2 is that the behaviour of the smallest scales are still under debate. For that reason the illustration simply an approximation. Integrating over the three different coloured curves it becomes obvious that they detect different amounts of kinetic energy. This can be seen directly in the figure, as every integral is the area beneath its respective curve. Obviously, the red curve, representing DYNAD with the tightest grid distance out of the three data sets, covers the largest part of the energy spectrum, then follows the green curve and the blue curve corresponding to HIRLAM and ERA-Interim respectively. Thus, Figure 2 illustrates the theory behind equation E1. Recall that in the Introduction section it is written that a model needs several grid cells in order to describe phenomena. Then it would be interesting to examine the kinetic energy for different resolutions. In this study, such a comparison was done for 1, 6 and 10 times the grid distances of the three data sets.

2.3 Data Analysis

Look again at the equations E3 and E5. Lindborg (1998) found an expression for the one-dimensional energy spectrum:

$$E(k) = d_1 k^{-5/3} + d_2 k^{-3} \quad (\text{E6})$$

In equation E6, Lindborg (1998) has defined the constants d_1 and d_2 as follows:

$$d_1 = C_0 |\Pi_u|^{2/3} = 9.1 * 10^{-4} \text{ m}^{4/3} \text{ s}^{-2}$$

$$d_2 = K \Pi_\omega^{2/3} = 3 * 10^{-10} \text{ s}^{-2}$$

Integrating equation E6 yields the kinetic energy of the energy spectrum:

$$\sigma^2(k) = \frac{3}{2} d_1 (k^{-2/3}) + \frac{1}{2} d_2 (k^{-2}) \quad (\text{E7})$$

Integrating between two wavenumbers k_1 and k_2 equation E7 becomes:

$$\sigma^2(k_1, k_2) = \frac{3}{2} d_1 (k_1^{-2/3} - k_2^{-2/3}) + \frac{1}{2} d_2 (k_1^{-2} - k_2^{-2}) \quad (\text{E8})$$

In equation E8 k_1 and k_2 are the wavenumber limits of the integral. Equation E8 is equation E7 with two wavenumbers compared. Substituting the wavenumber k_i with the wavelength $r_i = 1/k_i$ in equation E8 yields the variance with respect to wavelength:

$$\sigma^2(r_1, r_2) = \frac{3}{2} d_1 (r_1^{2/3} - r_2^{2/3}) + \frac{1}{2} d_2 (r_1^2 - r_2^2) \quad (\text{E9})$$

To see if the results of a study are significant to a certain percentage a significance test can be performed. A significance test is easily done by a one-sample t-test. Then a null hypothesis is first formed. In this study the kinetic energy calculated by different data sets were compared and the null hypothesis H_0 formulated was: $H_0: \bar{K}_i = \bar{K}_j$, where K_i and K_j are the kinetic energies calculated by two different models. Then the one-sample t -test is performed:

1. Define $\kappa = K_i - K_j$
2. Define the variance $S_\kappa^2 = \overline{(\kappa - \bar{\kappa})^2}$
3. Calculate the t -value:

$$t = \frac{\bar{\kappa}}{\sqrt{\frac{S_\kappa^2}{n_\kappa}}} \quad (\text{E10})$$

In equation E10 n_κ is the number of samples (in this study: number of time steps).

4. The t -value is compared to a reference table. That table can be found at the following website: <http://www.statsoft.com/textbook/distribution-tables/#t>

The t -value in the reference table depends on the degree of freedom and the p -value. The p -value is half the allowed percentage error and the degree of freedom is calculated by:

$$df = n_U - 1 \quad (\text{E11})$$

In the t-test the average difference is divided by the square root of the variance, i.e. the standard deviation. Thus, the larger the variance is, the lower the confidence.

2.4 The Storms Gudrun, Per and Carola

2.3.1 Gudrun, January 2005

The terrible storm Gudrun that caused seven deaths and 415 000 households without power is the most devastating storm to ever have struck Sweden. As cold air from Greenland streamed south out over the warmer water it mixed with mild and moist air north-west of the British Islands. In the frontiers between these two air masses a deep low pressure system was formed. At this point, a jet stream was present at higher altitude which caused enhanced divergence of the air in the top of the system. The enhanced divergence caused in turn an enhanced convergence of air at sea level which led to a quicker deepening of the pressure system. On mid-day, the 8th January, the low pressure system had travelled east and reached the south-western parts of Norway. It culminated during the night 8th-9th January when it passed Sweden (Figure 3). Just before passing the border of Norway and Sweden, the pressure was down to 960 hPa

(<http://www.smhi.se/kunskapsbanken/meteorologi/gudrun-januaristormen-2005-1.5300>, 2014-05-08).



Figure 3: The figure displays the path of the 2005 storm Gudrun measured at three hour time steps

(<http://www.smhi.se/kunskapsbanken/meteorologi/gudrun-januaristormen-2005-1.5300>, 2014-05-08).

2.3.2 Per, January 2007

Only one day before the storm Per struck Sweden it had formed just west of Scotland. In the early morning, the 14th January 2007, Per had travelled to Bergen on the Norwegian west coast. It then continued its journey east over Norway and eventually Sweden (Figure 4). Over the Swedish inland the strongest winds measured 29 m/s, while islands like Gotland and Hanö measured gusts of 34 and 40 m/s respectively

(<http://www.smhi.se/kunskapsbanken/meteorologi/per-januaristormen-2007-1.5287>, 2014-05-08).

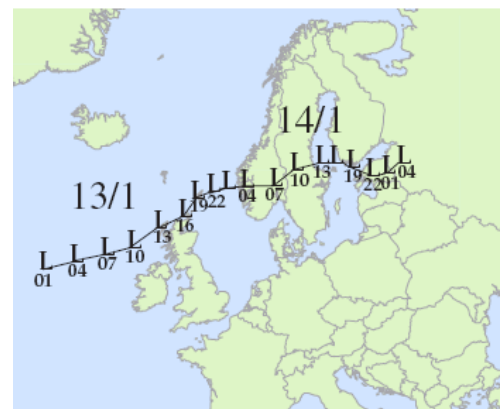


Figure 4: The figure displays the path of the 2007 storm Per in three hour time steps

(<http://www.smhi.se/kunskapsbanken/meteorologi/per-januaristormen-2007-1.5287>, 2014-05-08).

2.3.3 Carola, December 1999

In the turn of the months November to December in 1999 the southern parts of Sweden were struck by three storms in a row. The first one passed the 29th November. The strongest wind speeds measured 29 m/s. The second one came only one and a half day later with wind speeds of 25 m/s. Then it was time for Carola. It formed west of Ireland in the Atlantic Ocean the 2nd December and travelled east-north-east towards Denmark where it culminated on the evening the 3rd December. The pressure in its centre was then only 953 hPa. In Denmark the storm was called the storm of the century. During the night that followed the storm travelled over southern Sweden over the region called Götaland (Figure 5). At Falsterbo station the wind speeds measured 30 m/s and on the island Hanö, off the eastern coast of the region Skåne, wind speeds of 33 m/s were observed (<http://www.smhi.se/kunskapsbanken/meteorologi/hosten-1999-arhundradets-storm-1.5762>, 2014-05-08).

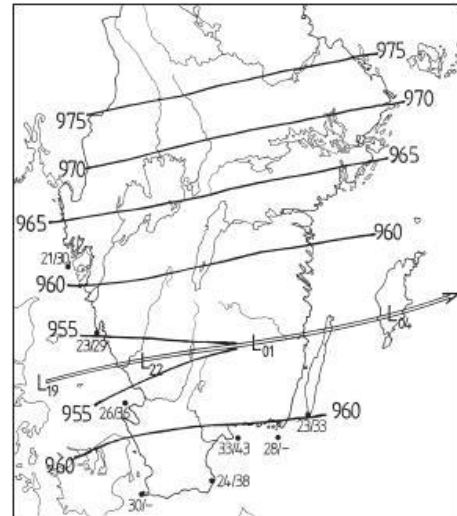


Figure 5: The figure displays the path of the 1999 storm Carola across Sweden. The numbers plotted in the figure are pressure values in hPa (<http://www.smhi.se/kunskapsbanken/meteorologi/hosten-1999-arhundradets-storm-1.5762>, 2014-05-08).

3. Method

Several codes were used to analyse the data for this study. Data were gathered from SMHI and ECMWF and the analyses were run on a supercomputer at NSC (National Supercomputing Centre) in Linköping.

The first three codes plotted the development of the storms Gudrun and Per by the three data sets DYNAD, HIRLAM and ERA-Interim. The region considered was the Nordic countries and the most northern parts of continental Europe.

Next, another code plotted the kinetic energy representation caught by each data set over a time series including a storm. The kinetic energy representation was plotted over the time intervals 1st January - 16th January 2005, 11th January - 16th January 2007 and 1st December - 6th December 1999 for the storms Gudrun, Per and Carola respectively. The kinetic energy representation was calculated over the storm affected region. That region covers the Swedish country parts Götaland and Svealand. As the density was constant (1 kg/m³), the mass part of the actual kinetic energy expression is ignored in the code and the kinetic energy is thus represented by

$$E_{kin} = \frac{1}{2}(u^2 + v^2) \quad (E12)$$

where u and v are the horizontal wind components at 10 meter height. The average kinetic energy was calculated over the region for four precise times per day (00, 06, 12 and 18).

Thereafter, observations made during the time of the storms were included in figures with wind speed representations. Three codes with different time intervals were used to plot these figures. The observational data were taken from the MORA-database at SMHI. Due to limited time in the study, data from only one measuring station could be used in the codes. The station chosen was Falsterbo on the south-western tip of Skåne, Sweden. The wind speed representation over the region was calculated over 16 and 21 days for the storms Gudrun and Per and 6 days for the storm Carola.

Then the mean kinetic energy for each storm was calculated. The mean kinetic energy was calculated over the storm affected region and over 16, 16 and 6 days for the storms Gudrun, Per and Carola respectively. The results are plotted in Table 1 in the Result section below.

Two kinetic energy calculations were made. The first was calculated with equation E7 and the wavenumbers used were those of the three data sets ERA-Interim ($1/80000 \text{ m}^{-1}$), HIRLAM ($1/22000 \text{ m}^{-1}$) and DYNAD ($1/5000 \text{ m}^{-1}$). The results are noted in Table 2. Then the variance in kinetic energy was calculated by equation E8 for three different effective resolutions; 1, 6 and 10 times the grid distance. The results are plotted in Table 3 in the Result section below.

Finally, a significance test was performed in the form of the one-sample *t*-test. The results of the one-sample *t*-test were compared to a reference value, i.e. the threshold of the *t*-test explained in the Theory section above. The reference value was determined by the degree of freedom and the *p*-value. The degree of freedom was 63 (because n_U in equation E11 was 64). The *p*-value was 0.025. The results from the significance test are plotted in Table 4.

4. Results

4.1 Development of the 2005 Storm Gudrun

Figure 6 illustrates the development of the 2005 storm Gudrun. The colourbar on the right of every figure displays the wind speeds over the region. The storm is the red area located in the North Sea, approaching Skagerrak, at noon the 8th January 2005. The following hours the storm approaches Scandinavia from south-east, striking the southern parts of Sweden in the afternoon and continues its journey east during the night. At midnight, the 9th January the storm has weakened and passed Scandinavia. Figure 6 was mostly constructed to give the reader an idea of the storm Gudrun. However, note the impact of land surface friction on the wind speeds as the storm crosses southern Sweden. With the colours, and the colourbar as a reference, it is easy to see the differences between wind speeds over areas with low and high friction, water and land respectively. That is, over land the friction is much greater than at seas, and so the winds are weaker over land than at seas.

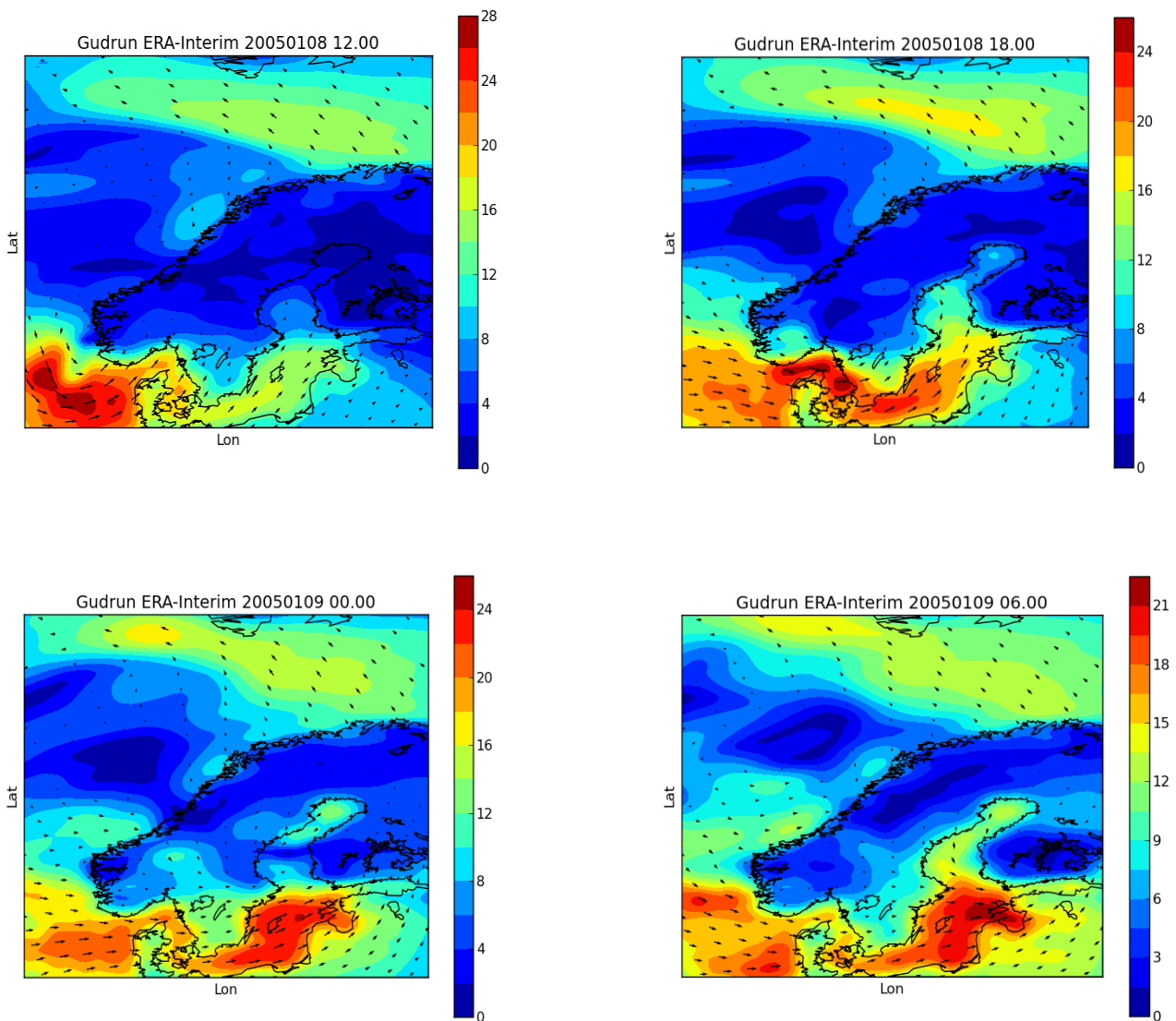


Figure 6: The figures display the development of the 2005 storm Gudrun by the data set ERA-Interim from 12.00 UTC 8th January 2005 to 06.00 UTC 9th 2005 in a six hour interval. The colourbar indicates wind speed in m/s.

4.2 Kinetic Energy Representations

In Figure 7 the kinetic energy representation of the three data sets DYNAD, HIRLAM and ERA-Interim is illustrated in a six hour interval from midnight the 31st December 2004 to 18.00 UTC the 16th January 2005. The storm Gudrun hit Sweden the 8th January 2005 and is displayed by the high middle peak. During the time of the storm the lines representing the data sets are organized as expected to equation E1, even though the difference between HIRLAM and ERA-Interim might be negligibly small, while before and after the time of the storm, the lines are not. From the way the lines are organized in Figure 7 the hypothesis cannot be proven.

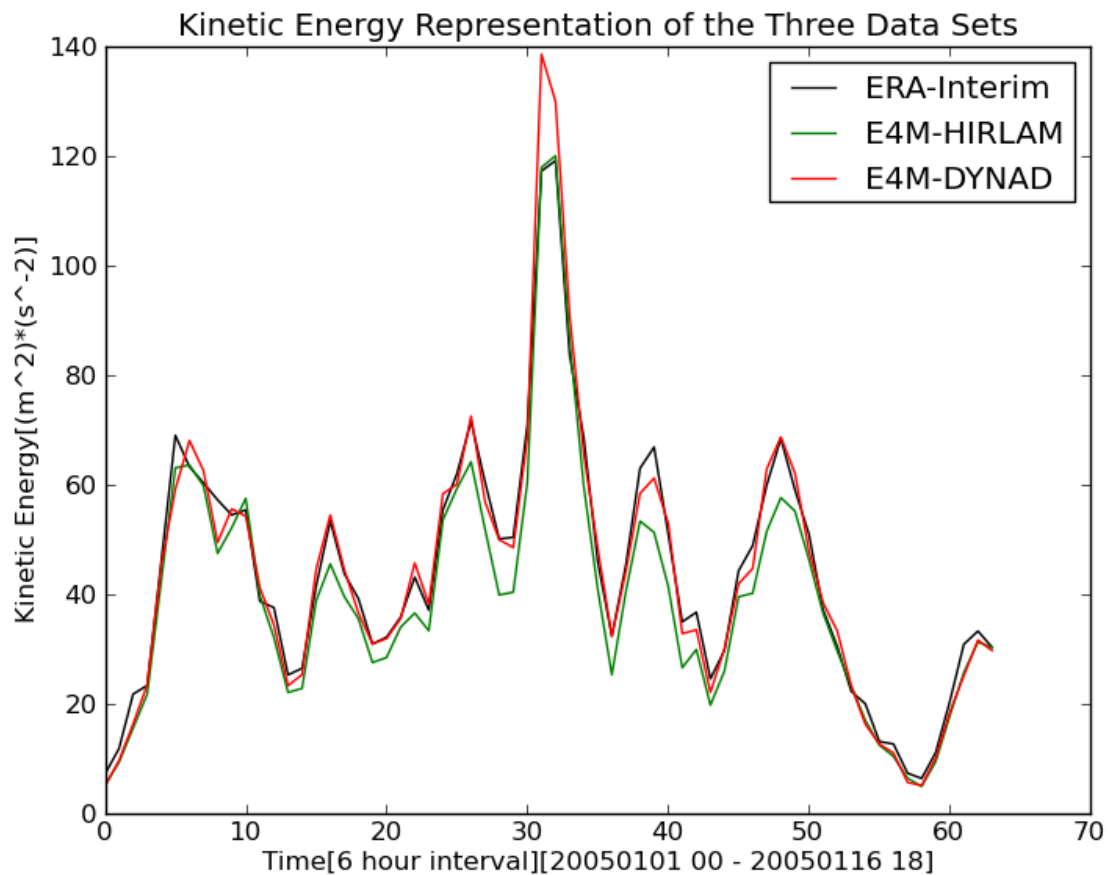


Figure 7: The figure displays the kinetic energy representation of the three data sets HIRLAM and DYNAD of the EURO4M project and ERA-Interim during the storm Gudrun. ERA-Interim (80 km grid) is represented by the blue line, HIRLAM in EURO4M (22 km grid) is represented by the green line and DYNAD in EURO4M (5 km grid) is represented by the red line.

In Figure 8 the kinetic energy representation of the three models DYNAD, HIRLAM and ERA-Interim is illustrated in a six hour interval from midnight the 6th January to 18.00 the 10th January 2005. The figure is a closer plot of Gudrun than Figure 7. In Figure 8 the kinetic energy representation is plotted for two days before to two days after the storm hit Sweden. It is even more apparent that during the time of the storm the lines representing the data sets are organized as expected to equation E1, while before and after the time of the storm, the lines are not, with the plot that is Figure 8.

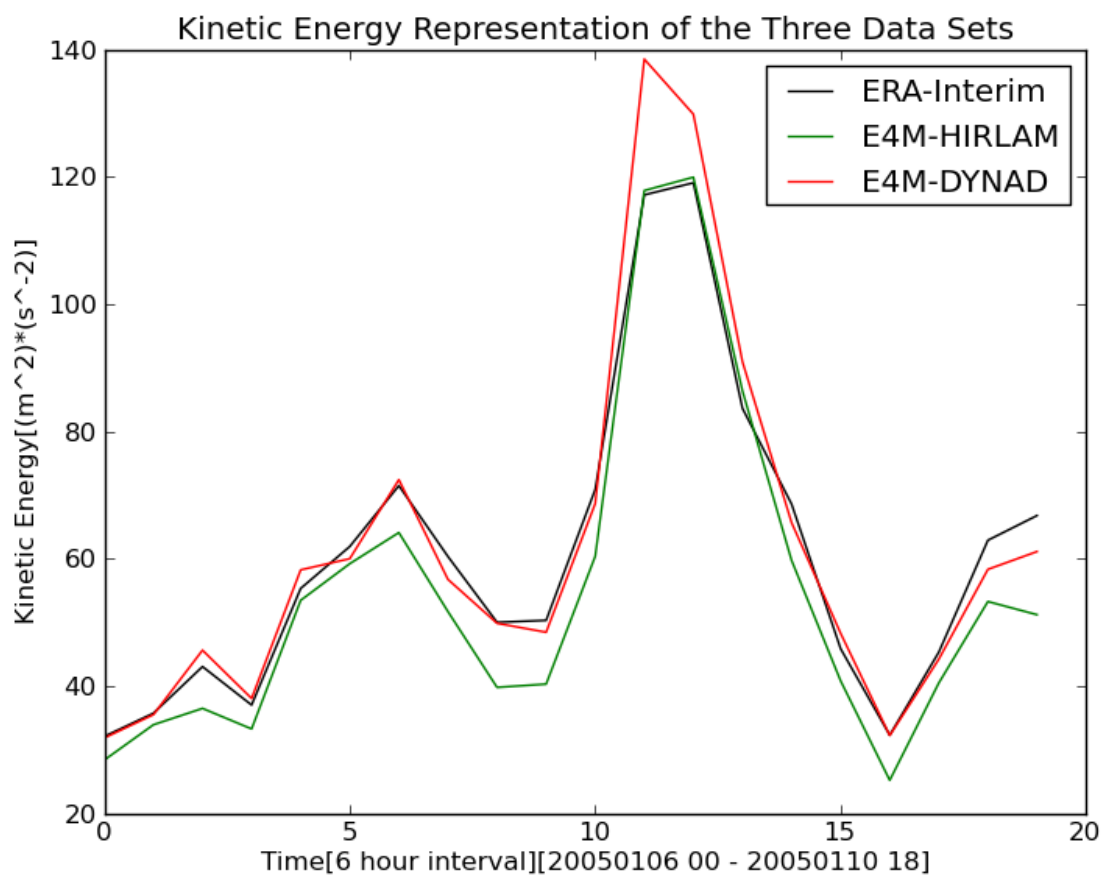


Figure 8: This is the same figure as Figure 7, but zoomed in on the six days around the storm Gudrun (from 00.00 the 6th January to 18.00 the 10th January).

In Figure 9 the kinetic energy representation of the three data sets DYNAD, HIRLAM and ERA-Interim is illustrated in a six hour interval from midnight the 11th January 2007 to 18.00 the 16th January 2007. The storm Per that hit Sweden the 14th January 2007 is displayed in the figure by the highest middle peak. Just like Figure 8 was a closer plot of the days before and after Gudrun, Figure 9 is a close plot of Per. The kinetic energy representation is only plotted for three days before to two days after the storm hit Sweden. During the time of the storm the lines representing the data sets are organized as expected to equation E1, while before and after the time of the storm, the lines are not. The hypothesis cannot be proven for this event either.

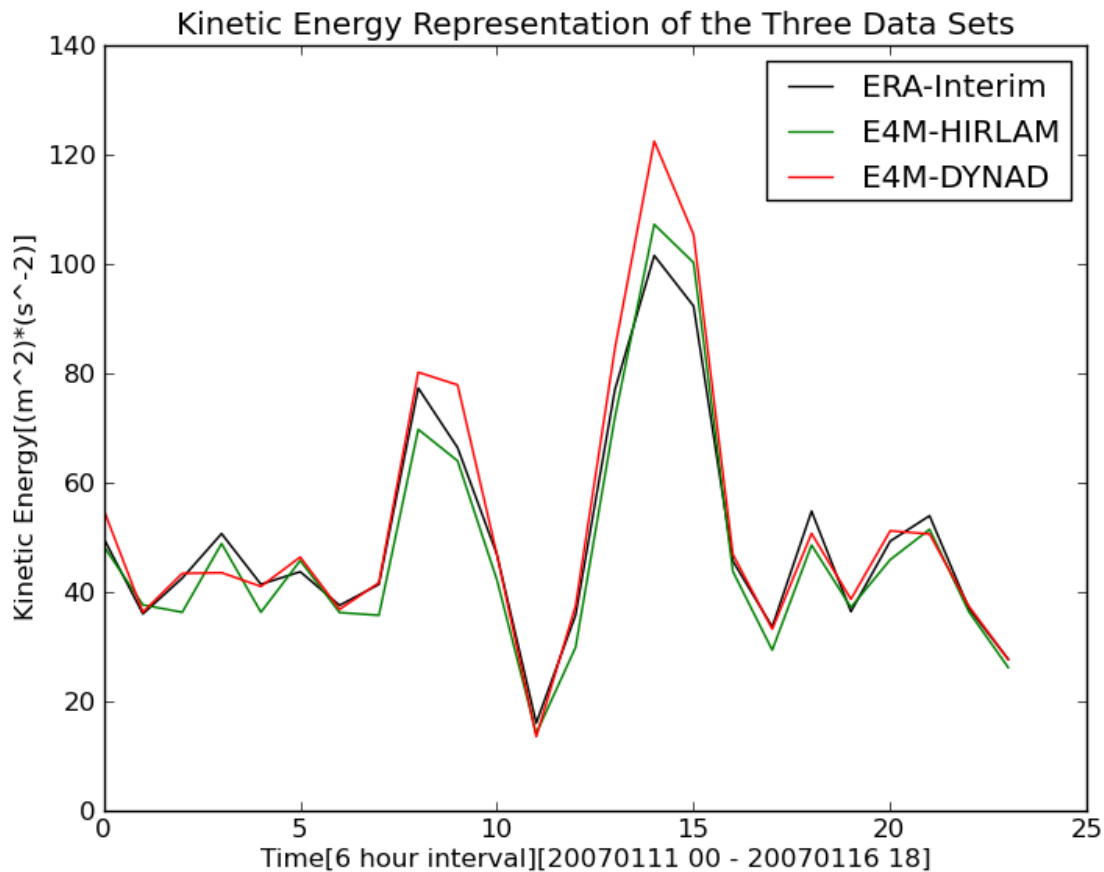


Figure 9: The figure displays the kinetic energy representation of the three data sets HIRLAM and DYNAD of the EURO4M project and ERA-Interim during the 2007 storm Per. ERA-Interim (80 km grid) is represented by the blue line, HIRLAM in EURO4M (22 km grid) is represented by the green line and finally DYNAD in EURO4M (5 km grid) is represented by the red line.

In Figure 10 the kinetic energy representation of the three data sets DYNAD, HIRLAM and ERA-Interim is illustrated in a six hour interval from midnight the 1st December 1999 to 18.00 UTC the 6th December 1999. The storm Carola hit Sweden the night between the 3rd and the 4th December 1999. The storm is displayed in the figure by the middle peak. Just like Figure 8 was a closer plot of the days before and after Gudrun, Figure 9 is a close plot of Carola. The kinetic energy representation is only plotted for two days before to two days after the storm hit Sweden. During the time of the storm the lines representing the data sets are organized as expected to equation E1, while before and after the time of the storm, the lines are not. So, the hypothesis cannot be proven for the Carola event either.

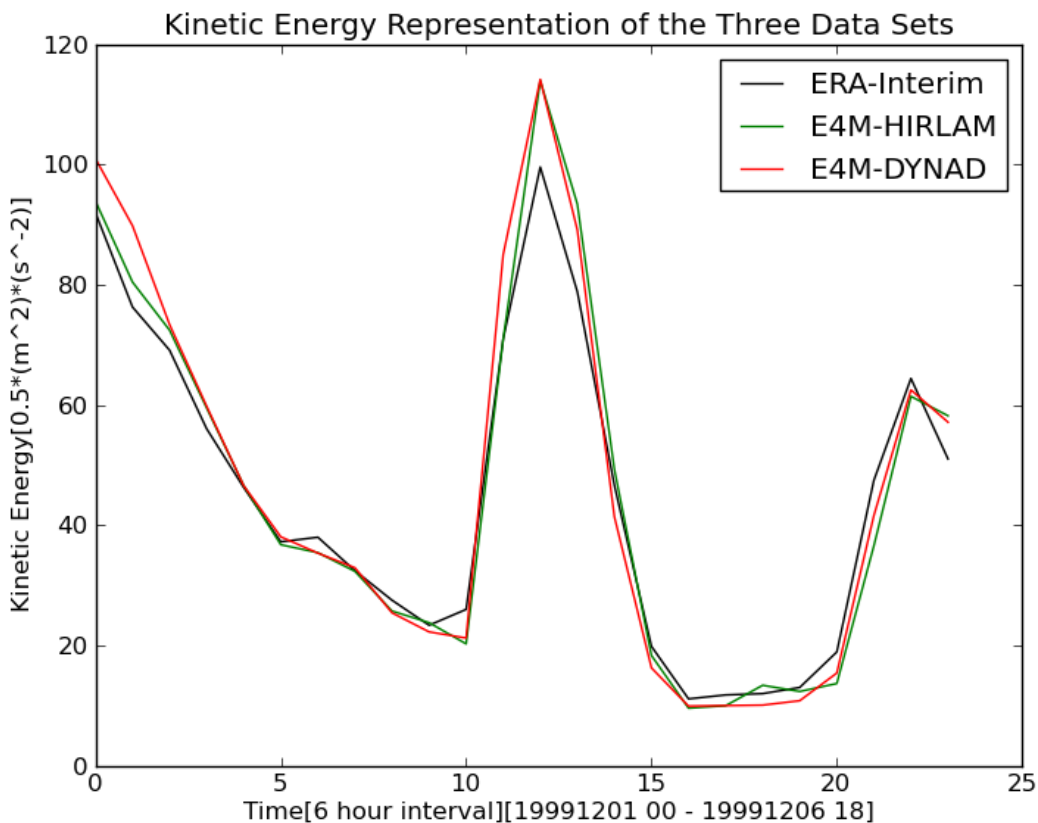


Figure 10: The figure displays the kinetic energy representation of the three data sets HIRLAM and DYNAD of the EURO4M project and ERA-Interim during the 1999 storm Carola. ERA-Interim (80 km grid) is represented by the blue line, HIRLAM in EURO4M (22 km grid) is represented by the green line and finally DYNAD in EURO4M (5 km grid) is represented by the red line.

4.3 Observation Comparisons

In Figure 11 the velocity representation of observations made at Falsterbo and the three data sets DYNAD, HIRLAM and ERA-Interim is illustrated in a six hour interval from midnight the 31st December 2004 to 18.00 UTC the 16th January 2005. The storm Gudrun hit Sweden the 8th January 2005 and is displayed by the high middle peak. In the figure, the line representing the observations generally lies beneath the other lines. That was not expected. The line representing observations was expected to lie above all three lines representing the data sets at all times.

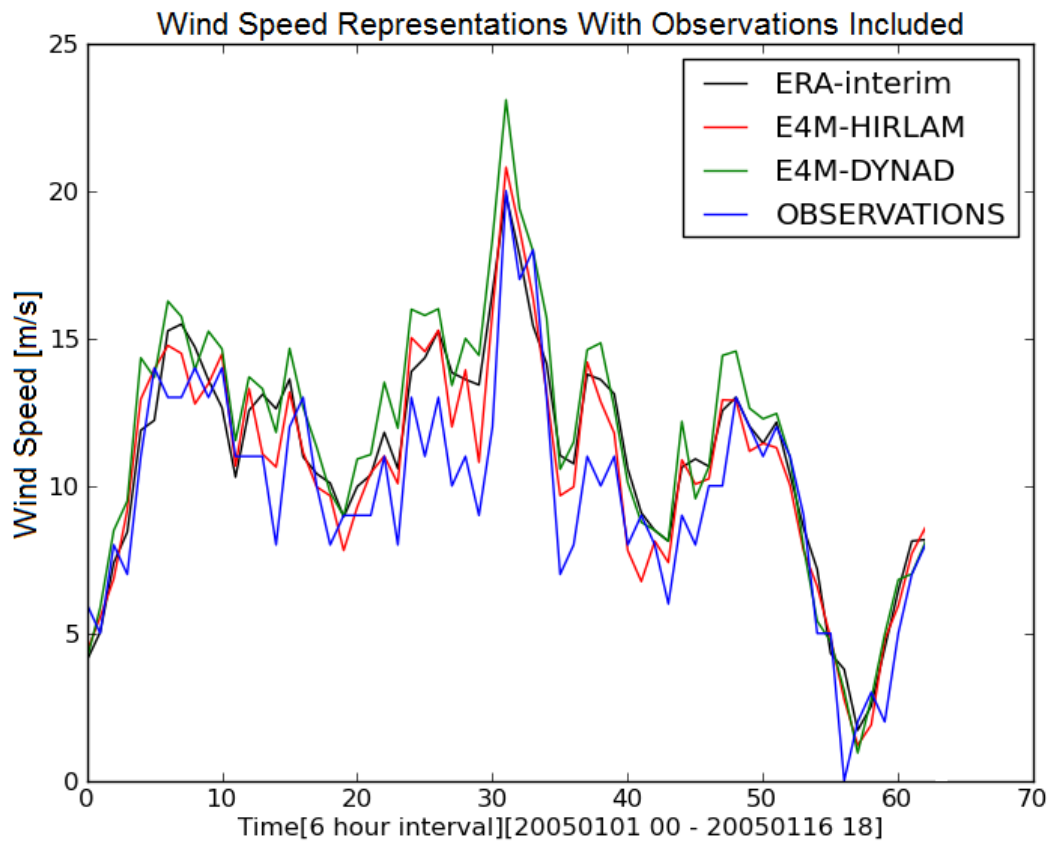


Figure 11: The figure displays the wind speed representations of the three data sets HIRLAM and DYNAD of the EURO4M project and ERA-Interim at the station Falsterbo. The blue line represents observations made at in Falsterbo during the storm Gudrun. The ERA-Interim model (80 km grid) is represented by the black line, the HIRLAM model in EURO4M (22 km grid) is represented by the red line the DYNAD model in EURO4M (5 km grid) is represented by the green line.

In Figure 12 the wind speeds of observations made at Falsterbo and the three data sets DYNAD, HIRLAM and ERA-Interim are illustrated in a six hour interval from midnight the 31st December 2006 to 18.00 UTC the 21th January 2007. The storm Per hit Sweden the 14th January 2007 and is displayed in the figure by the highest middle peak. In this figure the line representing the observations varies much between representing the highest wind speed at one time to representing the lowest at another time. Again, the line representing the observations was expected to lie above the lines representing the data sets at all times. In Figure 12 the main interest lies with the relative placement of the observations and the data sets, but as the kinetic energy representation of the storm Per was only plotted for six days in Figure 9, Figure 12 also works as an illustration of the relative placement of the data sets. Figure 12 shows that the hypothesis cannot be proven for the event of storm Per.

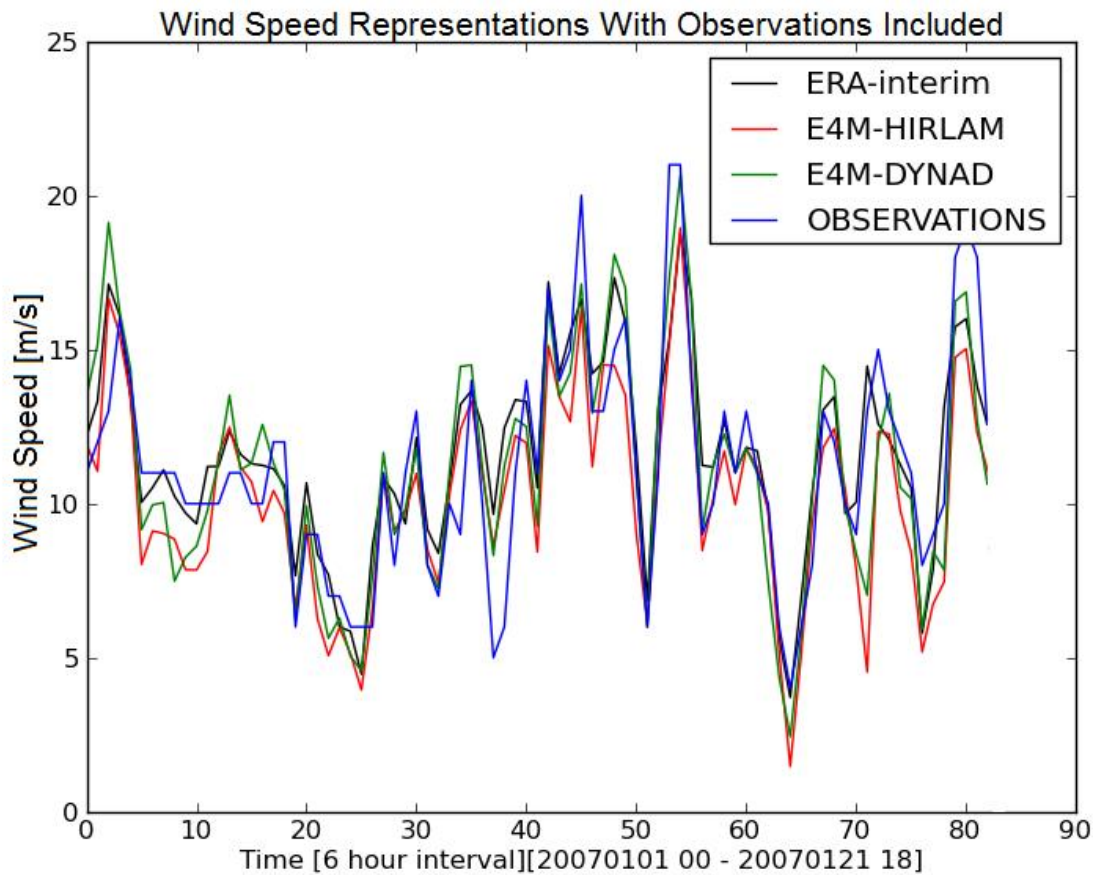


Figure 12: The figure displays the wind speed representations of the three data sets HIRLAM and DYNAD of the EURO4M project and ERA-Interim at the station Falsterbo. The blue line represents observations made at Falsterbo during the storm Per. The ERA-Interim model (80 km grid) is represented by the black line, the HIRLAM model in EURO4M (22 km grid) is represented by the red line the DYNAD model in EURO4M (5 km grid) is represented by the green line.

Figure 13 that displays the wind speed representations of Carola is the same image as Figure 9 (which displayed the kinetic energy representations of Carola), but with wind speeds plotted instead of kinetic energy and with the addition of observations plotted as a line of reference. Again, the line representing the observations was expected to lie above all three lines representing the data sets at all times, but instead it varies much, representing anything between the highest and lowest kinetic energies.

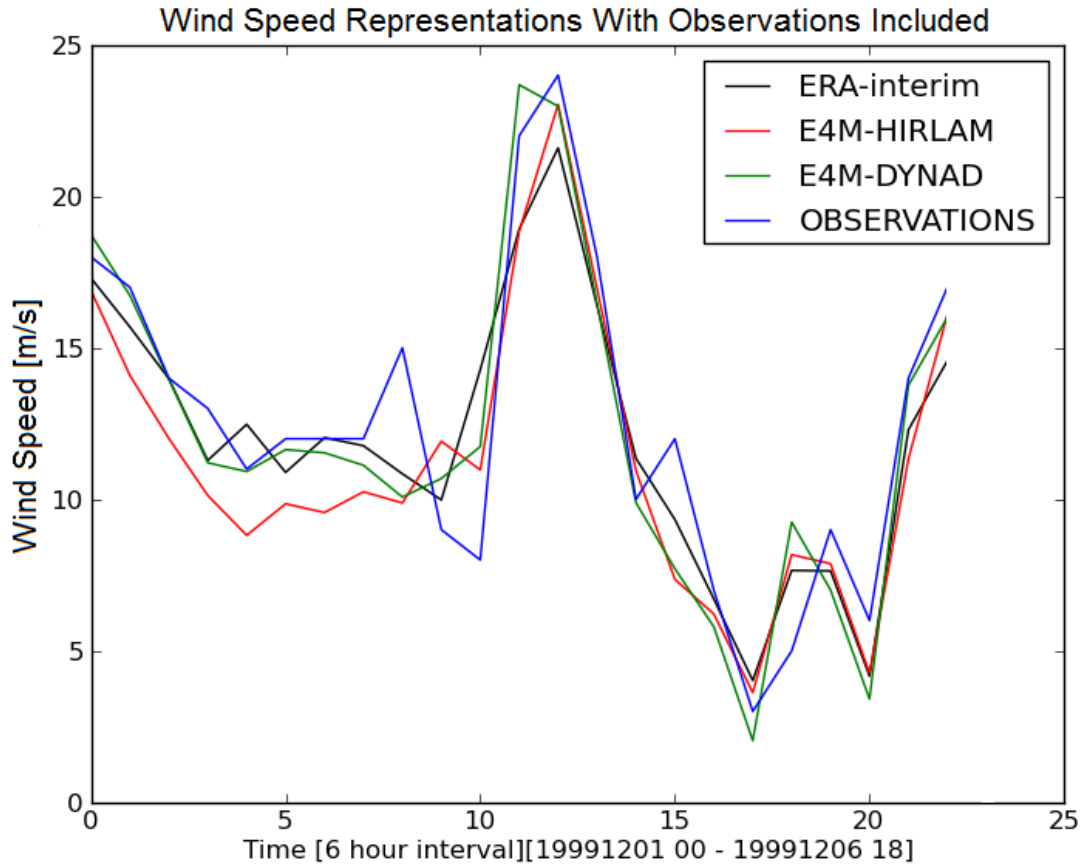


Figure 13: The figure displays the wind speed representations of the three data sets HIRLAM and DYNAD of the EURO4M project and ERA-Interim at the station Falsterbo. The blue line represents observations made at in Falsterbo during the storm Carola. The ERA-Interim model (80 km grid) is represented by the black line, the HIRLAM model in EURO4M (22 km grid) is represented by the red line, the DYNAD model in EURO4M (5 km grid) is represented by the green line.

4.4 Mean Kinetic Energy- and Theoretical Calculations

In Table 1 the calculated mean kinetic energy for each model is plotted. For every storm DYNAD catches the most energy across the whole region, but in two out of three events (Gudrun and Per), ERA-Interim catches more kinetic energy than HIRLAM. The only time where HIRLAM has caught more energy than ERA-Interim is during the Carola event. The Carola time series was only run for six days, while Gudrun and Per were run for 16 days respectively. Once again, the results cannot prove the relation of equation E1.

Table 1: The table displays the mean kinetic energy averaged over the area described in the Method section calculated. The time period of each storm is noted below the names of each storm.

Storm/Data Set	ERA-Interim (80 km)	HIRLAM (22 km)	DYNAD (5 km)
Gudrun [m²s⁻²] 1 st Jan. – 16 th Jan. 2005	40.93	39.45	43.40
Per [m²s⁻²] 1 st Jan. – 16 th Jan. 2007	39.72	37.35	40.63
Carola [m²s⁻²] 1 st Dec. – 6 th Dec. 1999	44.60	45.37	46.24

4.5 Kinetic Energy

In Table 2 the kinetic energy calculated with equation E7 is plotted. This is the energy which is not described by the respective grid distance of the data set. The values in Table 2 are to be compared with those plotted in Table 1 above. The kinetic energy values could be interpreted as the margin of error, or as a value of how variable the kinetic energy values of Table 1 are.

Table 2: The table displays the kinetic energy calculated by equation E7.

	80 000 m	22 000 m	5000 m
Kinetic Energy [m²s⁻²]	3.49	1.14	0.40

In Table 3 the kinetic energy of two compared data sets is calculated by equation E8 for 1, 6 and 10 times the grid distances. The values could also be interpreted as the average differences in kinetic energy between two data sets plotted for different effective resolutions.

In Table 4 the variance is interpreted as the margin of error of the average difference.

Table 3: The table displays the kinetic energy calculated by equation E8. The respective grid distances are again 80, 22 and 5 km for ERA-Interim, HIRLAM and DYNAD. The different effective resolutions compared are 1, 6 and 10 times the grid distance.

	$k_1=80\,000\text{ m}^{-1}$; $k_2=22\,000\text{ m}^{-1}$	$k_1=80\,000\text{ m}^{-1}$; $k_2=5000\text{ m}^{-1}$	$k_1=22\,000\text{ m}^{-1}$; $k_2=5000\text{ m}^{-1}$
1 times the grid distance [m²s⁻²]	2.35	3.09	0.74
6 times the grid distance [m²s⁻²]	36.68	41.48	4.70
10 times the grid distance [m²s⁻²]	95.53	105.54	10.01

The wind amplitudes corresponding to the values in Table 3 could be calculated by taking the square root of the values in Table 3 multiplied with 2.

4.6 Significance Test

The calculated t -values of Table 4 are to be compared with the threshold value 1.95996. The threshold value is the one corresponding to the infinite degree of freedom and the p -value of 0.025. From values higher than the threshold value there is 95 % chance that the average difference between two data sets is not zero. Analogously, there is still a 5 % risk that the average difference is zero. In Table 4 five out of nine values are higher than the threshold value. All t -values for the storm Gudrun are higher than the threshold value, whilst none of the t -values for the storm Carola are higher than the threshold value.

Table 4: The table displays the t -values calculated to perform the significance test for each storm. The respective grid distances are again 80, 22 and 5 km for ERA-Interim, HIRLAM and DYNAD.

	ERA-Interim vs. HIRLAM	ERA-Interim vs. DYNAD	HIRLAM vs. DYNAD
Gudrun	2.95333	3.69951	7.60550
Per	5.31617	1.66920	6.32825
Carola	0.68770	1.29414	0.98363

5. Discussion

5.1 Figures Describing Kinetic Energy Representations

From the figures Figure 7 and Figure 8 it is obvious that the theory of equation E1 in the theory section could not be confirmed by this study, i.e. the lines representing the three data sets are not always organized with DYNAD above HIRLAM, which in turn lie above ERA-Interim, as predicted by equation E1. An important observation to note in Figure 8 is that the only time when equation E1 holds is at the time of the storm. Grasping for the discovery that the hypothesis holds for events of particularly strong winds to be true, it was tested for another storm, the 2007 storm Per.

The observation that the lines are organized as predicted by equation E1 holds for the 2007 storm Per as well (Figure 9). When discussing Figure 9 it should be noted that it too shows an irregular disorder and overlap of the lines before and after the storm, just as the Figures 7 and 8. Especially interesting to note is that the lines are not organized as predicted by the theory during the event of rather strong winds two days before Per. That observation makes it harder to prove that the thesis equation (equation E1) holds for events of particularly strong winds. Furthermore, the tendencies of disordered lines are also found when plotting the 1999 storm Carola (Figure 10). When studying Figure 10, it should be noted that the differences in the lines representing DYNAD and HIRLAM are negligibly small during the most intense storming. Now, Carola was obviously preceded by another strong wind event during the month shift 30th November to 1st December. That event is not completely included in Figure 10, because the code designed to plot the figure is limited to only allow events to occur during one and the same month. Nevertheless, during the part of that particular event which is visible in Figure 10, the lines are organized as expected from equation E1.

That raises the ultimate question of this study; why do the lines in the figures organize themselves in random orders, according to equation E1, during events of particularly strong winds? The chaos, or disorder, that rules between the lines in the figures Figure 7, 8 and 10 before and after the storms, could perhaps be explained by the low wind speeds. It might be that the wind speeds during these events are low enough for errors to be of significant importance. That could explain the disorder that rules during these events. That reasoning leads on to another important question to consider; what errors are found in this study and these data sets? In general, many of the errors of a NWP-model lie within the variables parameterised. One such variable yet to be tested is friction. Friction is parameterised by the surface roughness length in the models and the roughness lengths differ between the models. At higher altitudes, when the impact of friction on the wind is negligible, the hypothesis (equation E1) might be valid. For such a study DYNAD cannot be used as it has no vertical extensions. DYNAD calculates only the horizontal 10 metre wind, but still such a study could be performed with data from HIRLAM and ERA-Interim. So that could be a future study.

The kinetic energy is represented by half the metre per second squared. Thus, the value of the horizontal velocity is the square root of the double kinetic energy value (equation E13 below).

$$E_{kin} = \frac{1}{2}v^2 \quad \Rightarrow \quad v = \sqrt{2E_{kin}} \quad (E13)$$

Now look, for instance, at Figure 8. It appears as if, during the most intense storming, the models differ quite a lot, and in the expected order. DYNAD plots a value of $140 \text{ m}^2\text{s}^{-2}$ while HIRLAM and ERA-Interim plot values close to $118 \text{ m}^2\text{s}^{-2}$ respectively. Roughly calculating the velocity plotted by each model the respective results are 16.7, 15.4 and 15.4 m/s. Elementary, the velocity magnitude difference, roughly calculated from the kinetic energy representation in Figure 8, is significantly smaller than the magnitude difference between the corresponding kinetic energy representations. These roughly calculated velocity values should not be compared with the velocity values of Figure 8, as the velocity values in Figure 11 are plotted for one station, while the kinetic energy representations of Figure 8 are plotted for the entire storm region (Götaland and Svealand).

Considering all the figures plotted in this study, the Gudrun event (Figure 8), is the event with the largest difference between the models. Then, it is also the event with the largest velocity difference. The two lines furthest apart are the ones representing DYNAD and ERA-Interim and that difference is 1.9 m/s. Now consider the disorders between the lines occurring before and after each storm in any figure during almost any given event. There are apparent disorders, but as the lines lie even closer together during these events than during the actual storm events, they could be considered to agree with each other to a good accuracy. Keep in mind that it is their plotted kinetic energy representation that appears to agree to a good accuracy in the figures and then imagine how well their velocity representations must agree. The fact that the data sets depend on each other, i.e. as HIRLAM uses ERA-Interim as boundary conditions and that DYNAD is a dynamic downscaling of HIRLAM, is a reason to believe that the differences between the data sets perhaps should be expected to be small. Looking at the figures describing the kinetic energy representations there are often clear mutual trends when considering all the lines as one. What is meant by these trends is that the data sets often display similar events, even though their values might differ. Perhaps those trends could be considered an argument that the lines do agree to a “small” difference. To conclude this paragraph, it could be that what this study has proven is that the wind programs of the three data sets DYNAD, HIRLAM and ERA-Interim are in rough agreement with each other.

Concerning wind speeds, it could be interesting to discuss storm damages. Storm damage estimates are proportional to the wind speed cubed (v^3). With the roughly calculated wind speeds of the second last paragraph, DYNAD 29 percent more storm damage than HIRLAM and ERA-Interim. Storm damage reports are of great importance to society and accurate reports are of course always preferred. Then, the discussion has returned to which data set is the most accurate.

It is always important to be aware of the flaws in a study. The aim of this particular study was, as mentioned earlier, to verify the relation assumed in equation E1. In this study the relation could not be verified by wind analysis. A very crucial point to discuss is then whether the wind was a good parameter to begin with analysing. Perhaps the relation could have been

verified by analysing another parameter, like temperature, cloudiness or precipitation (to name a few). Of course, if an analysis was made considering another parameter, DYNAD could not have been used as it only calculates the wind. However, the real interest of this study was to evaluate if data sets using tighter grid distance catch more information than those with wider. All the relation of equation E1 is based on is the very reasonable assumption that the data collected by a data set increases with a tighter grid distance. Of course, for this assumption to be true, it should be possible to prove by wind analysis too. It should also be commented that out of the four parameters mentioned in this paragraph (wind, temperature, cloudiness and precipitation) wind and temperature are generally the parameters that any model predicts most accurately. Actually, temperature might be predicted a little more accurately than wind. A reasonable question would thus be why temperature was not examined? It could be in future studies, but here wind was chosen to be examined because the theory of the power laws is rather well accepted.

Forecast data is another thing that could be examined. In this study, analysis data was examined, which is the result of the data assimilation procedure. As such, the analysis is a statistical result. Forecast data are pure model states that fulfill the dynamical equations of the atmosphere. Thus, forecast data should follow the observed power laws for the kinetic energy.

5.2 Observation Comparisons

The observations were included as a reference to the three data sets. Theoretically, the observations would be the truth, i.e. they were included to plot the precise wind velocities during the plotted events and the line representing the observations was thus expected to always lie above the lines representing the three data sets. Obviously, that is not the case. The simple explanation to this is believed to be that Falsterbo was a poor selection of station. Falsterbo was chosen because it lies on the south-western tip of Sweden. The station lies on a peninsula and is almost completely surrounded by water. Falsterbo was chosen as it was one of the stations exposed to the strongest winds during the three storm events (Gudrun, Per and Carola). However, the fact that Falsterbo is completely surrounded by water is also the reason why it was a poor selection. One of the things parameterised in models and data sets are boundary conditions, e.g. coastlines. Because Falsterbo lies on a slim peninsula, the models parameterise the peninsula to be considered as the ocean. Thus, the models anticipate stronger winds over Falsterbo than those actually measured. Hence, the lines representing the observations are not always above the lines representing the data sets. In fact, they often lie beneath all three data sets. Furthermore, Falsterbo station is only one place, while the data of the data sets represents entire grid boxes. Finally, it should be mentioned that observations are not without error. For example, stations might stand close to trees blocking the wind or the instruments may break. That should not be the case, but it might happen anyway.

5.3 Mean Kinetic Energies, Variance and Significance Test

The mean kinetic energy calculated over the storm affected region (Götaland and Svealand) was calculated as another way of comparing the data sets. Now, bear in mind that the values in Table 1 are not to be compared with values found at a particular point, but is merely the mean kinetic energy found by each data set across the storm affected region. It was expected that the values of Table 1 would obey the relation of equation E1, but apparently they do not.

Furthermore, it is obvious from Table 1 that for every storm DYNAD catches the most energy across the whole region, but in two out of three events, ERA-Interim catches more kinetic energy than HIRLAM. The only time where HIRLAM has caught more energy than ERA-Interim is during the Carola event. However, the Carola time series was only run for six days, while Gudrun and Per were run for 16 days. Once again, the study failed to prove the relation of equation E1. It could be discussed whether there would be a significant difference between the results if the storms were all run for the same time series. The longer the time series, the more credible the average value would be. Thus, it might be that the hypothesis would hold if the time series run would have been an entire month, i.e. that HIRLAM actually catches more energy than ERA-Interim, as the hypothesis suggests.

Look again at Table 4. The one-sample *t*-test was performed to evaluate the probability of the mean kinetic energy of two compared data sets not being equal to zero. Five out of nine values are larger than the threshold value. That is to say that those values indicate 95 % chance that the average difference between two compared data sets is not zero. A probable reason to why none of the values for Carola are higher than the threshold value is that the Carola time series run was only six days. However, this explanation was never tested. When performing a one-sample *t*-test, the differences become important. As noted in the Theory section, higher factors are needed to create larger values in theoretical difference. It could be that the effective resolution of ERA-Interim and HIRLAM is coarser than 10 times the grid distance.

5.4 Criticism of the References Used

The references used to gather facts needed for this study must be considered credible sources. The facts are gathered from university literature or peer-reviewed articles and studies written by devoted authors. The internet pages used as sources are also to be considered credible. The internet pages are from the European Centre of Medium-Range Weather Forecasts (ECMWF), the Swedish Institute of Meteorology and Hydrology (SMHI) and the homepage of the EURO4M project.

6. Conclusion

In this study it was examined whether tighter grid means that more weather is caught. The hypothesis was then applied to wind analysis. The hypothesis could not be verified by this study. It would seem as if it holds for events with particularly strong winds, but it could not be proven for events with weak winds. The one-sample *t*-test showed that the average difference in kinetic energy of two different data sets were to 95 % probability not zero. Future studies are needed to evaluate the hypothesis. A good thing to remember then is to choose a better station as reference. If future studies show that the hypothesis holds it should be evaluated for other weather parameters as well before it can be considered proven.

7. References

1. Dahlgren, P., Kållberg, P., Landelius, T., Undén, P., “D 2.9 “D 2.9 Comparison of the Regional Reanalysis Products with Newly Developed and Existing State-of-the Art Systems”, EURO4M Project – Report, January 2014
2. Kraichnan, R. H., “Inertial Ranges in 2 dimensional turbulence”, *Physics of Fluids*, vol.10, p.1417, 1967
3. Lautrup, B., “Physics of Continuous Matter”, Second Edition, CRC Press, Taylor and Francis Group, Boca Raton, p. 253, 2011
4. Lilly, D. K., “Two-dimensional Turbulence Generated by Energy Sources at Two Scales”, *Journal of Atmospheric Science*, vol. 46, p. 2026-2030, 1989
5. Lindborg, E., “Can the atmospheric kinetic energy spectrum be explained by two-dimensional turbulence?”, Department of Mechanics, KTH, Stockholm, Sweden, 1998
6. Nastrom, G. D., Gage K. S., Jasperson, W. H., “Kinetic energy spectrum of large- and mesoscale atmospheric processes”, *Nature* 310, vol. 310, p. 36-38, 1984
7. Smith, L. M., Yakhot, V., “Finite-size Effects in Forced Two-dimensional Turbulence”, *Journal of Fluid Mechanics*, vol. 274, p. 115-138, 1994
8. <http://www.ecmwf.int/en/forecasts/datasets/era-interim-dataset-january-1979-present>, 2014-05-09
9. <http://www.ecmwf.int/research/era/do/get/era-interim>, 2014-04-14
10. <http://www.euro4m.eu/>, 2014-04-03
11. <http://www.smhi.se/kunskapsbanken/meteorologi/gudrun-januaristormen-2005-1.5300>, 2014-05-08
12. <http://www.smhi.se/kunskapsbanken/meteorologi/hosten-1999-arhundradets-storm-1.5762>, 2014-05-08
13. <http://www.smhi.se/kunskapsbanken/meteorologi/per-januaristormen-2007-1.5287>, 2014-05-08